

# Thermodynamic Analysis for a Solar-Driven Combined Heating and Power System Under Libyan Climatic Conditions

Salah Khalefa ABORAGIGA

<sup>1</sup>Corresponding Author: Department of Mechanical Engineering, Faculty of Engineering, Karabük University, 78050 Karabük, Turkey

## ABSTRACT

*This study investigates the performance of a solar-powered Combined Cooling, Heating, and Power (CCHP) system designed specifically for the climate of Tripoli, Libya. With the country's high solar potential and the pressing need for sustainable energy solutions, this system combines a regenerative Brayton cycle with a lithium bromide–water absorption cooling unit to maximize energy efficiency. Solar energy is captured using a heliostat field and concentrated on a central receiver to heat air, which then drives a turbine to generate electricity. The remaining thermal energy is used for both heating and cooling applications, allowing the system to meet multiple energy demands simultaneously. A thermodynamic model was developed to evaluate the system under steady-state conditions, using realistic local climate data. The results for the month of June indicate a net electrical output of 5761 kW, along with 2424 kW of heating and 7603 kW of cooling. The system achieved an energy utilization factor of 73.41% and an exergy utilization factor of 36.83%. Electrical energy and exergy efficiencies were recorded at 26.8% and 29.6%, respectively, while the coefficient of performance (COP) of the absorption cooling unit was 0.82. What sets this work apart is its focus on Libya's specific environmental conditions, which are often overlooked in existing research. The findings highlight the potential of solar-powered CCHP systems to improve energy sustainability in sun-rich, high-temperature regions and offer valuable insights for future renewable energy planning in similar contexts.*

**KEYWORDS;**- Combined Cooling Heating and Power (CCHP); Regenerative Brayton cycle; Absorption refrigeration; Libya.

Date of Submission: 12-05-2025

Date of acceptance: 26-05-2025

## I. INTRODUCTION

With fossil fuel resources steadily declining and environmental concerns on the rise, there has been a growing shift toward renewable energy systems. Technologies that make use of solar and biomass energy have attracted considerable interest in recent years, thanks to their sustainability and low environmental impact [1], [2]. Among these, Combined Cooling, Heating, and Power (CCHP) systems are gaining attention for their ability to improve energy efficiency by producing electricity, heating, and cooling simultaneously within a single system [3][4]. When powered by renewable sources like solar energy, CCHP systems not only reduce dependence on fossil fuels but also help cut greenhouse gas emissions [5]. Libya, in particular, benefits from abundant solar radiation, positioning it as a strong candidate for solar energy-based solutions [6]. However, the efficiency of such systems is closely tied to local weather conditions, including temperature, humidity, and solar intensity, which can vary significantly. For this reason, evaluating the thermodynamic performance of a solar-CCHP system under Libyan climatic conditions is essential to understanding its viability and optimizing its design for real-world application[7], [8].

In recent years, significant research has been devoted to solar-powered CCHP systems; however, studies specifically addressing the unique climatic conditions of Libya remain limited. For example, Ai et al. [9] proposed a novel CCHP system integrating solar thermal energy with an Organic Flash Cycle (CCHP-ST-OFC) that outperforms conventional and ORC-based systems, offering higher electricity and heat output, improved exergy (38.7%) and energy efficiency (53.1%), and 9% lower natural gas consumption. Akroot et al. [10] analyzed a solar-powered tri-generation system achieving 232.5 kW electricity, 86.89% thermal efficiency, and 0.195 kgCO<sub>2</sub>/kWh carbon footprint. The system showed strong exergoeconomic performance with a cost rate of 66.12 \$/h. Han et al. [11] optimized a CO<sub>2</sub>-based combined heating and power system, achieving a minimum exergy-environmental cost of 0.387 \$/kWh and significant efficiency gains. Xu et al. [12] proposed a solar-powered system combining liquid dehumidification and absorption refrigeration for year-round use in China.

Yadav et al. [13] presented an improved solar-driven cooling and power system with 33% higher performance and 44% greater exergy efficiency than standalone systems. It also reduces cost and CO<sub>2</sub> emissions by up to 38% and 26%. Saini et al. [14] introduced a solar-driven CCHP system for remote buildings that achieves 3.16% exergy efficiency, lowers costs, and reduces CO<sub>2</sub> emissions. It performs best with higher generator or evaporator temperatures and is suitable for future sustainable energy needs. Akroot et al. [15] address Libya's dependency on traditional fuels by proposing a hybrid solar-based Integrated Solar Combined Cycle (ISCC) system using the Sarir power plant as a case study to highlight the potential of ISCC to support sustainable energy transitions in Libya and similar oil-producing nations. Wang et al. [16] optimized a solar-driven CCHP system using a flat-plate collector and thermal storage, combining an ORC with an ejector refrigeration cycle. Yan et al. [17] proposed a hybrid solar-assisted CCHP system using a phosphoric acid fuel cell and natural gas reforming. Wu et al. [18] optimized a solar-assisted steam/air biomass gasification CCHP system, achieving 51.34% efficiency and offering improved thermal performance and energy reliability over conventional systems. Yang et al. [19] proposed a solar-driven SCO<sub>2</sub>-based CCHP system with 79.75% energy and 58.63% exergy efficiency. It achieves 85.04% energy savings, 86.05% emission reduction, and a low electricity cost of 10.4 ¢/kWh.

Despite the growing body of literature on solar-powered CCHP systems, there remains a distinct gap in studies tailored to Libya's unique solar and climatic conditions. This work addresses that gap by developing and analyzing a novel solar-driven CCHP configuration specifically optimized for Tripoli, Libya. It incorporates a regenerative Brayton cycle integrated with a LiBr–H<sub>2</sub>O absorption cooling system and uses actual solar irradiance data to assess performance. Unlike prior studies that mainly focus on generalized or non-Libyan contexts, this study provides a comprehensive thermodynamic, energy, and exergy evaluation under real-world Libyan environmental conditions, thereby offering practical insights for the implementation of renewable energy solutions in the region.

## II. MODEL DESCRIPTION

Figure 1 illustrates a Solar-Driven Combined Cooling, Heating, and Power (CCHP) System operating in Tripoli, Libya. This is a hybrid energy system that integrates solar thermal power with absorption-based cooling and heating. Solar radiation is collected by heliostats and focused on the receiver to heat air. The hot air expands in a turbine to generate power. The turbine exhaust heat is reused in the recuperator and absorption cycle. Some of the waste heat is diverted to a heater to provide hot water for domestic or industrial use. The remaining heat is used in the generator to drive an absorption refrigeration cycle (LiBr–H<sub>2</sub>O), producing chilled air for cooling. The solar subsystem in the proposed CCHP system consists of key components designed to efficiently convert solar energy into thermal energy for power generation. The process begins with the heliostat field, which comprises an array of mirrors that track the sun and reflect its rays onto a central solar receiver. This receiver absorbs the concentrated solar radiation and transfers the thermal energy to a working fluid, typically air or another suitable gas. The heated, high-pressure working fluid then flows into a turbine, where it expands and generates mechanical power that can be converted into electricity. To enhance system efficiency, a recuperator is employed to recover a portion of the waste heat from the turbine exhaust and use it to preheat the compressed air before it enters the receiver. This reduces the energy required for heating the fluid, thus improving the overall thermal performance. The subsystem also includes a compressor that draws in ambient air and compresses it to a higher pressure, subsequently directing it through the recuperator and into the receiver. The heating subsystem in the solar-powered CCHP configuration is responsible for utilizing a portion of the available waste heat to meet thermal energy demands, specifically for hot water production. This is achieved through the use of a heater that extracts waste heat from the working fluid between thermodynamic points 7 and 9. The recovered heat is then transferred to water or another heat transfer fluid to generate hot water at point 10, which can be used for space heating or domestic applications, thereby contributing to the high overall energy efficiency of the system. The cooling subsystem of the proposed CCHP system employs a LiBr–H<sub>2</sub>O absorption chiller loop to produce cooling by utilizing low-grade heat recovered from the turbine exhaust. The process begins in the generator, where thermal energy from point 6 drives the separation of the refrigerant (water vapor) from the absorbent (LiBr solution). The system incorporates a solution heat exchanger (SHEX) to improve thermal efficiency by transferring heat between the strong and weak solution streams. The weak solution is pressurized by a pump before entering the generator, reducing the energy input requirement. In the absorber, the refrigerant vapor is reabsorbed into the strong LiBr solution, releasing heat, while the evaporator generates cooling by evaporating water under low pressure. Finally, the condenser liquefies the vapor refrigerant, completing the cycle.



**III. THERMODYNAMICS MODEL**

The primary objective of the thermodynamic analysis is to evaluate the energy and exergy efficiencies of the system. The mass, energy and exergy balance equations for each component are outlined as follows [20], [21], [22]:

$$\sum \dot{m}_i = \sum \dot{m}_e \tag{1}$$

$$\sum \dot{m}_i x_i = \sum \dot{m}_e x_e \tag{2}$$

$$\dot{Q} + \sum \dot{m}_i h_i = \dot{W} + \sum \dot{m}_e h_e \tag{3}$$

$$\dot{E}x_Q + \sum \dot{m}_i ex_i = \dot{E}x_w + \sum \dot{m}_e ex_e + \dot{E}x_{dest} \tag{4}$$

$$\dot{E}x_Q = \left(1 - \frac{T_o}{T_k}\right) \dot{Q}_k \tag{5}$$

$$\dot{E}x_w = \dot{W} \tag{5}$$

The solar energy intercepted in the mirrors is determined by the direct normal intensity ( $I_{DNI}$ ) projected area of the mirror ( $A_a$ ), and optical efficiency ( $\eta_{opt}$ ), which is given by [23], [24]:

$$\dot{Q}_{solar} = \eta_{opt} * A_a * I_{DNI} \tag{7}$$

The electrical energy efficiency and overall energy efficiency of the CCHP system are calculated from the following equations:

$$\eta_{I,electrical} = \frac{\dot{W}_{net}}{\dot{Q}_{solar}} \tag{8}$$

$$\eta_{I,CCHP} = \frac{\dot{W}_{net} + \dot{Q}_{heating} + \dot{Q}_{cooling}}{\dot{Q}_{solar}} \tag{9}$$

The electrical exergy efficiency and overall exergy efficiency of the CCHP system are calculated from the following equations:

$$\eta_{II,electrical} = \frac{\dot{W}_{net} + \dot{Q}_{heating} + \dot{Q}_{cooling}}{\dot{E}x_{Q_{solar}}} \tag{10}$$

$$\eta_{II,CCHP} = \frac{\dot{W}_{net}}{\dot{E}x_{Q_{solar}}} \tag{11}$$

Also, the coefficient of performance (COP) of the absorption refrigeration system is calculated from the following equations:

$$COP = \frac{\dot{Q}_{Evap}}{\dot{Q}_{Gen} + \dot{W}_P} \tag{3-15}$$

**IV. RESULTS AND DISCUSSION**

Table 2 provides the thermodynamic properties at various state points of the solar-powered CCHP system, including pressure, temperature, and enthalpy values essential for performance analysis.

State	Mass (kg/s)	Pressure (bar)	Temperature (°C)	Enthalpy (kJ/kg)	Enthalpy (kJ/kg · K)
1	45	1	303	303.5	5.716
2	45	8	597.2	604.4	5.811
3	45	8	647.2	657.2	5.895
4	45	8	1077	1135	6.46
5	45	1	693	706.1	6.565
6	45	1	626.1	634.9	6.457
7	45	1	426.1	427.8	6.06
8	45	1	373	374	5.925
9	12.87	1	303	125.2	0.4347
10	12.87	1	348	313.5	1.014
11	22.31	0.008634	310	81.92	0.238
12	22.31	0.06944	310.2	81.92	0.238
13	22.31	0.06944	344	153.8	0.4579
14	19.08	0.06944	360	217.7	0.4764
15	19.08	0.06944	331.1	163.6	0.3196
16	19.08	0.008634	321.6	163.6	0.3197

17	3.239	0.06944	360	2654	7.519
18	3.239	0.06944	312	162.7	0.557
19	3.239	0.008634	278	162.7	0.586
20	3.239	0.008634	278	2510	9.029
21	193.1	1	303	125.2	0.4347
22	193.1	1	313	167	0.5704
23	450.9	1	303	125.2	0.4347
24	450.9	1	308	146.1	0.5031
25	121.2	1	303	125.2	0.4347
26	121.2	1	288	62.45	0.2223

Table 2. Thermodynamic properties at different states for the solar-powered CCHP system

Table 3 presents the energy and exergy performance of the solar-powered CCHP system in June, showing a net power output of 5761 kW, a heating load of 2424 kW, and a high cooling load of 7603 kW. The energy utilization factor reaches 73.41%, while the exergy utilization factor is 36.83%. Additionally, the system achieves an electrical energy efficiency of 26.8%, an exergy efficiency of 29.6%, and a COP of 0.82 for the absorption refrigeration system, confirming its suitability for hot climates like Tripoli, Libya.

Aspect	Symbol	Value
Net power output (kW)	$\dot{W}_{net}$	5761
Heating load (kW)	$\dot{Q}_{heating}$	2424
Cooling Load (kW)	$\dot{Q}_{cooling}$	7603
CCHP energy utilization factor (%)	$u_{I,CCHP}$	73.41
CCHP exergy utilization factor (%)	$u_{II,CCHP}$	36.83
Electrical energy efficiency (%)	$\eta_{I,electrical}$	26.8
Electrical exergy efficiency (%)	$\eta_{II,electrical}$	29.6
Coefficient of Performance of ARS	COP	0.82

Table 3. Energy and Exergy Performance of solar-powered CCHP system in June.

Table 4 provides a detailed exergy analysis for each component of the solar-powered CCHP system, showing a total exergy destruction of 16.88 MW and an overall exergy efficiency of 36.38%. The solar receiver (SR) accounts for the highest exergy destruction at 44.41%, followed by the generator (Gen) and gas turbine (GT) with 11.36% and 9.7%. In contrast, components like the air compressor (AC), SHEX, and pump show high exergy efficiencies above 90%, demonstrating minimal losses.

Component	$\dot{E}_{destruction}$ (MW)	$\dot{E}_{destruction}$ (%)	Exergy efficiency (%)
Abs	1.239	8.33	5.85
AC	1.293	8.7	90.45
Cond	1.11	7.45	10.53
Ev1	0.028	0.19	86
Ev2	0.0006	0.00038	87
Evap	0.523	3.52	59.62
Gen	1.69	11.36	56.65
GT	1.443	9.7	93.04
Heater	0.422	2.84	27.98
Pump	0	0	100
Rec	0.513	3.45	70.37
SHEX	0.008	0.05	93.8
SR	6.606	44.41	67.65
Total	16.88	100	36.38

Table 4. Exergy analysis for each component of the solar-powered CCHP system

Figure 2 illustrates the variation of three key output parameters, net work output, cooling load, and heating load, as a function of the pressure ratio in a solar-driven CCHP system. The findings present that Pressure ratio optimization is crucial in improving system performance, particularly for heating and power production. The net power output and heating load benefit significantly from increased pressure ratios, while the cooling load shows marginal gain. System designers should consider these trends when aiming to maximize total energy

utilization, especially in climates or seasons where heating demand is high. The net work output curve shows a clear increasing trend in net work output as the pressure ratio rises from 7 to 13. The work output increases from 5285 kW at PR = 7 to 6281 kW at PR = 13, showing an 18.8% improvement. This trend indicates enhanced power generation efficiency due to higher turbine pressure ratios, which increase the enthalpy drop across the turbine. The cooling load also increases steadily, but with a slower rate of change compared to the net work output. It rises from 7557 kW to 7682 kW, which is a 1.6% increase across the tested pressure ratio range. The relatively flat slope suggests that the cooling subsystem is less sensitive to pressure ratio variations. The results also indicate a significant and nearly linear increase in heating load with increasing pressure ratio. The heating load increases from 950.3 kW at PR = 7 to 4764 kW at PR = 13—approximately a fivefold increase. This steep rise can be attributed to the enhanced waste heat recovery at higher pressure ratios, improving the performance of the heating subsystem.

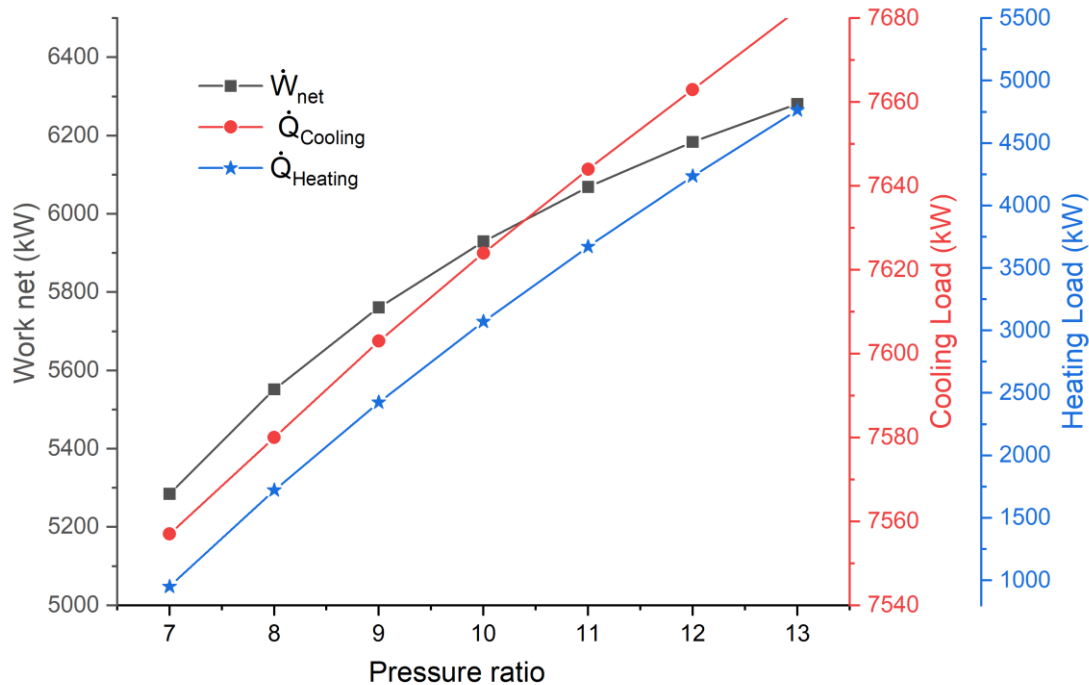


Figure 2. Effect of Pressure Ratio on Net Work Output, Cooling Load, and Heating Load in a Solar-Driven CCHP System

Figure 3 illustrates the influence of pressure ratio (ranging from 7 to 13) on the performance metrics of a solar-powered CCHP system operating in Tripoli, Libya. Increasing the pressure ratio significantly improves both electrical output and the overall energy and exergy efficiencies of the solar-assisted CCHP system. While the COP remains constant, indicating stable cooling performance, the gains in thermal and exergetic efficiency demonstrate the system's enhanced ability to convert and utilize available energy effectively. Both the first law and the second law electrical efficiencies show a steady increase with rising pressure ratio. At a pressure ratio of 7, the electrical exergy efficiency ( $\eta_{II}$ ) starts at 27.18% and increases to 32.31% at a pressure ratio of 13, marking a significant performance gain. This improvement results from higher turbine work output and better utilization of the high-pressure air in the Brayton cycle. Energy efficiency of the CCHP system increases from 64.13% to 87.08% across the pressure ratio range, showing a strong upward trend due to improved heat recovery and overall energy use. Also, the exergy efficiency of the CCHP system follows a similar trend, rising from 31.07% to 44.76%, indicating reduced system irreversibilities and better thermodynamic quality of the energy used. The COP remains constant at 0.8159 across all pressure ratios, indicating that the absorption cooling subsystem performance is independent of pressure ratio changes in the Brayton cycle. This is expected, as the COP of the LiBr-H<sub>2</sub>O system primarily depends on temperature levels rather than pressure ratios.

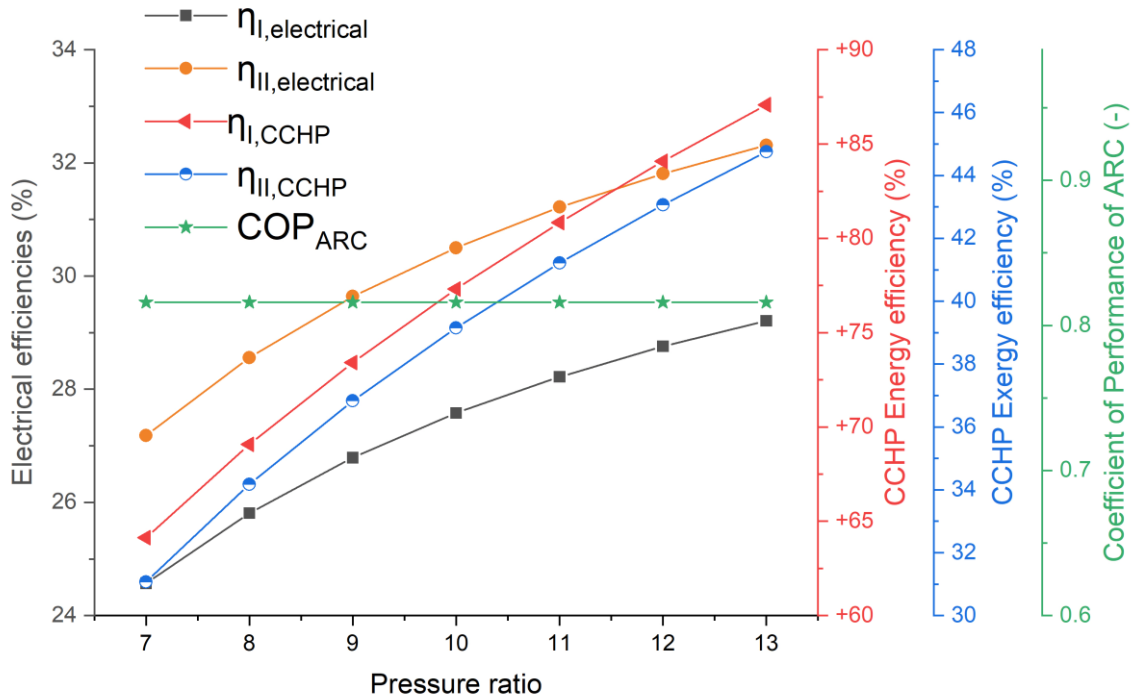


Figure 3. Effect of Pressure Ratio on Energy, Exergy, and Cooling Performance of the Solar-Driven CCHP System

Figure 4 illustrates the monthly average Direct Normal Irradiance (DNI) profile for Tripoli. The data shows a clear seasonal variation, with the highest DNI values—approximately 6.8–7.0 kWh/m<sup>2</sup>/day, occurring during the summer months (May to July). From March to October, DNI values consistently exceed 5.5 kWh/m<sup>2</sup>/day. In contrast, winter months such as December and January experience lower DNI values around 4.4–4.6 kWh/m<sup>2</sup>/day. This DNI pattern confirms that Tripoli has a strong solar resource, especially during the high-demand summer season, which aligns well with increased cooling needs.

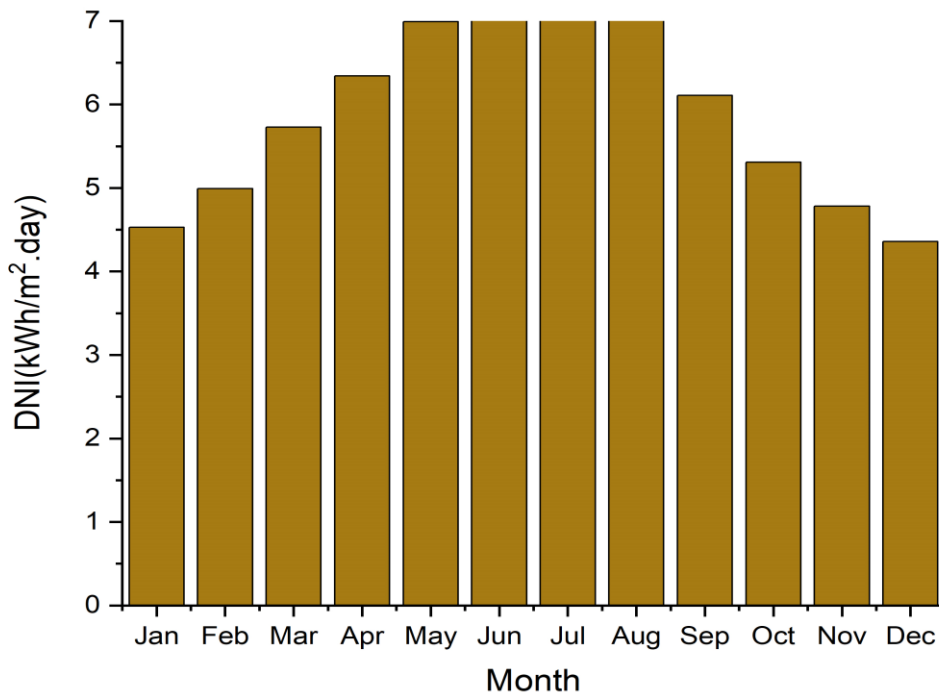


Figure 4. Monthly Variation of Direct Normal Irradiance (DNI) in Tripoli: Assessment of Solar Energy Availability Throughout the Year.

Figure 5 shows the monthly variation in net power output from the solar-assisted SA-CCHP system in Tripoli. The results clearly highlight the seasonal dependency of the SA-CCHP system. Its performance is strongest when solar input is high, making it especially suitable for summer-dominant climates like Libya, where cooling demand also peaks during this period. The highest net power output obtained in June–July, reaching around 6000–6200 kW, occurs during June and July. This corresponds with the period of maximum solar irradiance, as seen in Fig. 2, where DNI levels are at their peak (~7 kWh/m<sup>2</sup>/day). From January to May, the power output gradually increases from ~2500 kW to 5500 kW. This reflects the rising solar intensity during the spring and early summer months, enhancing the system’s performance and power generation capacity. After August, there is a steady decline in net power output, dropping to around 2600 kW in December, which matches the drop in DNI values during autumn and winter. This reduction is expected, as less thermal energy is available to drive the turbine efficiently.

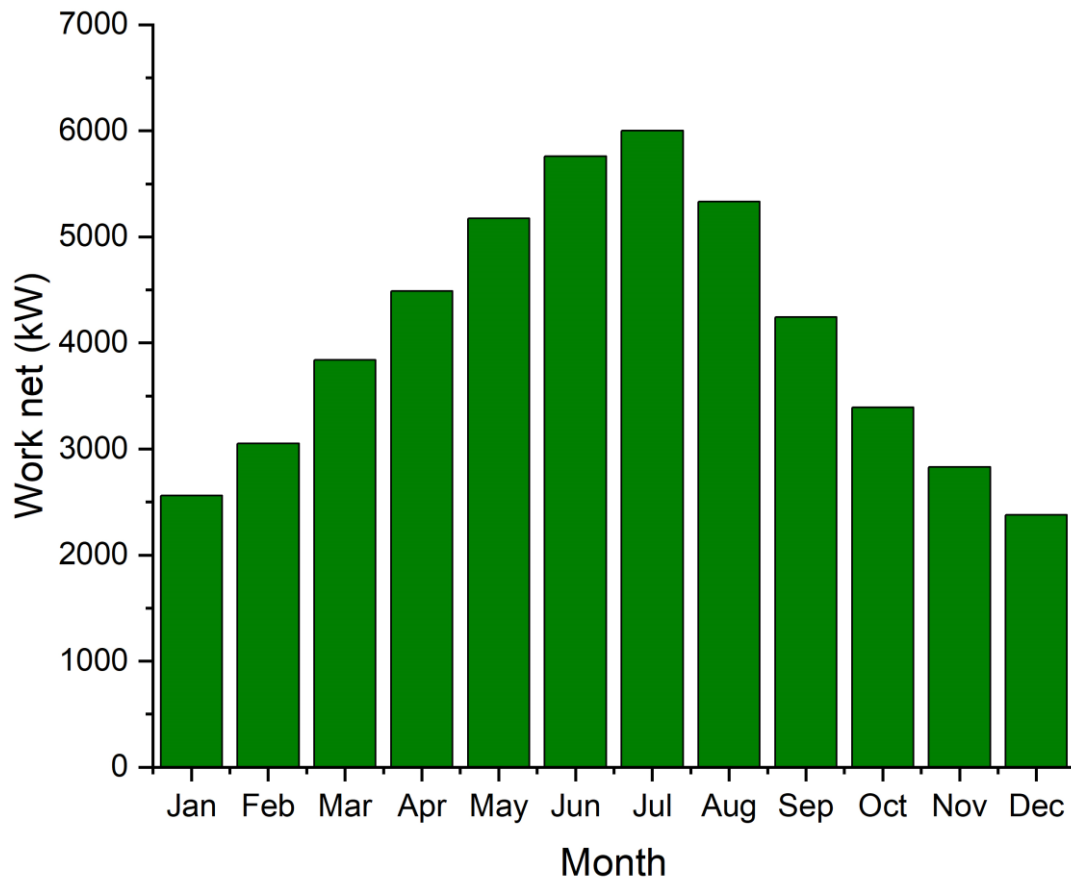


Figure 5. Monthly Net Power Output of the Solar-Assisted CCHP System in Tripoli.

Figure 6 illustrates the monthly variation in heating load delivered by the solar-assisted CCHP system in Tripoli. The heating output trends reveal a direct correlation with solar thermal energy availability and system efficiency throughout the year. Unlike conventional expectations, where heating demand is highest in winter, this figure represents available heating supply from the system, not demand. It highlights the seasonal variation in solar-driven thermal output, rather than user-side requirements. The heating load peaks at approximately 2600–2700 kW in June and July, which aligns with the maximum solar input period. This suggests the system makes effective use of high DNI values to produce surplus thermal energy for heating applications. From January (~750 kW) to June, there is a steady increase in heating output. This period benefits from rising solar irradiance and higher Brayton cycle temperatures, enhancing the waste heat recovery used for heating. Post-July, the heating load decreases, falling to about 650 kW in December. This reflects reduced thermal availability from the solar subsystem, and lower ambient temperatures reducing heating demand.

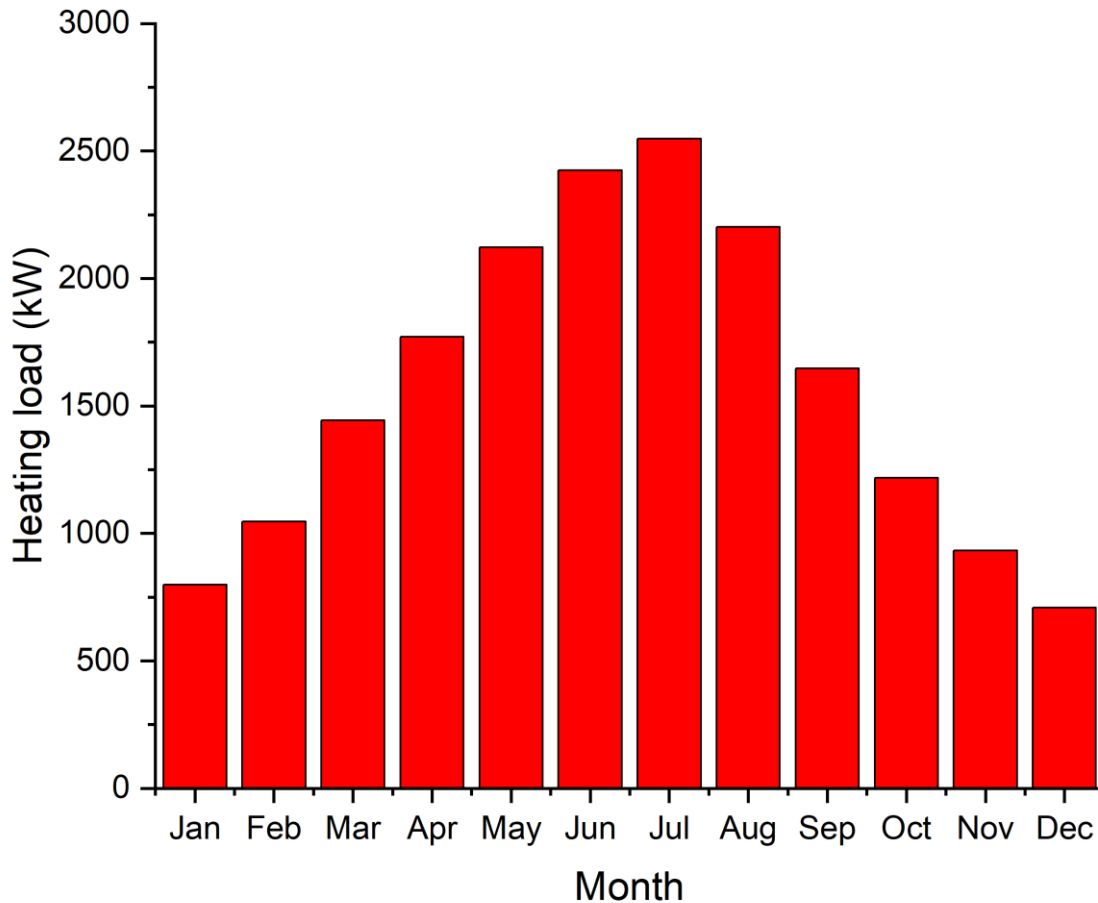


Figure 6. Monthly Heating Load Supplied by the SA-CCHP System in Tripoli.

Figure 7 displays the monthly cooling load delivered by the solar-assisted combined cooling, heating, and power (SA-CCHP) system in Tripoli. Despite seasonal variation, the difference between maximum and minimum cooling output is relatively small ( $\sim 70$  kW), which reflects the system's stable performance. This is especially important in climates like Tripoli, where cooling is needed for most of the year. The highest cooling load occurs in June and July, reaching up to approximately 7610 kW. This coincides with the peak of solar irradiance and ambient temperatures, indicating the system's ability to handle increased cooling demand during the hottest months. Starting from about 7550 kW in January, the cooling load gradually increases, showing the system's improved performance as more solar energy becomes available toward summer. After July, there's a slight but steady decline in the cooling load, dropping to around 7540 kW by December. This corresponds with reduced solar thermal input and likely reduced cooling demand in the cooler months.

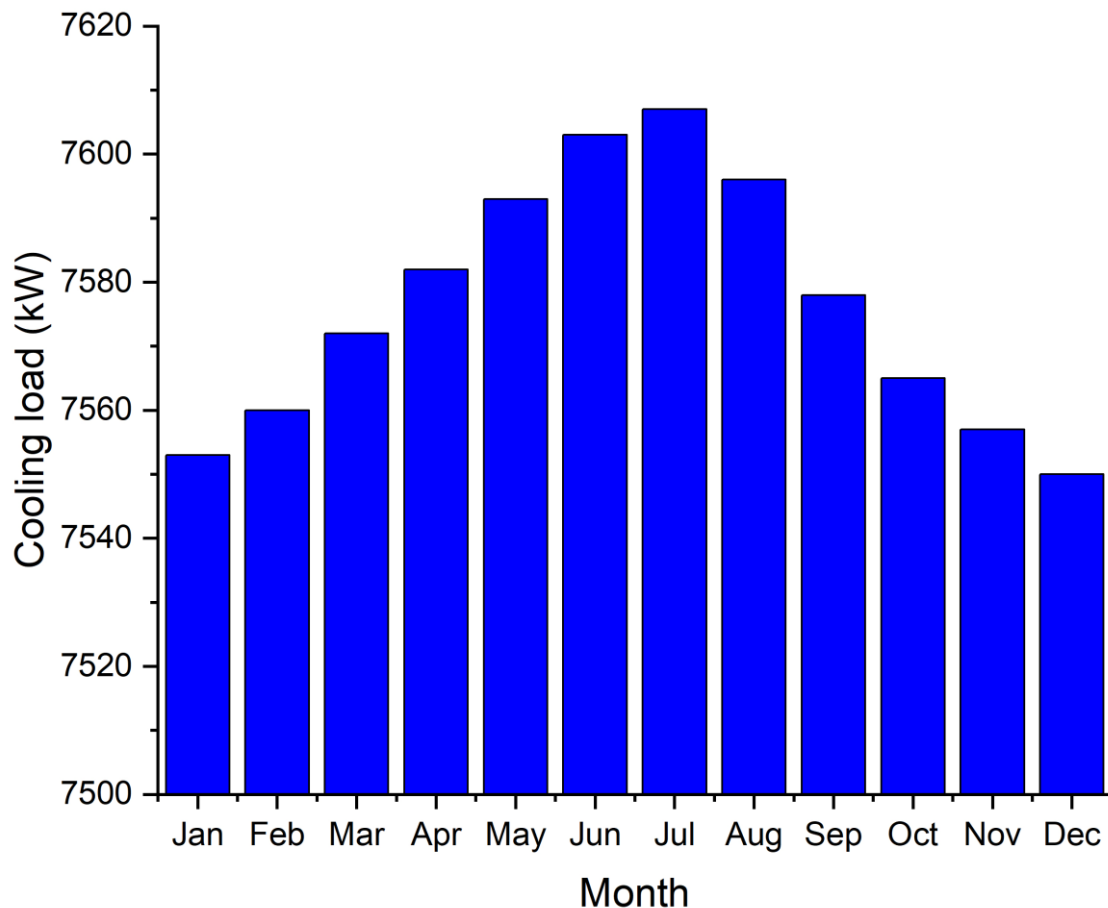


Figure 7. Monthly Variation of Cooling Load Supplied by the SA-CCHP System in Tripoli

## V. CONCLUSION

This research explored the feasibility and performance of a solar-powered CCHP system specifically designed for the environmental conditions in Tripoli, Libya. By combining a regenerative Brayton cycle with a lithium bromide–water absorption cooling system, the study aimed to make the most of Libya’s abundant solar resources to meet electricity, heating, and cooling demands more efficiently.

The results show that the system performs well under local climate conditions, especially during the summer months when solar radiation is at its peak. With notable outputs in power, heating, and cooling, and relatively high energy and exergy utilization rates, the system proves to be both efficient and adaptable. The absorption cooling loop, in particular, demonstrated strong performance, offering reliable cooling in a region where such demand is consistently high.

However, the exergy analysis pointed to the solar receiver as a key area where energy losses are most significant, highlighting the need for design improvements to further enhance overall efficiency. Despite this, the system as a whole shows strong promise for addressing energy challenges in Libya, offering a cleaner and more sustainable alternative to conventional fossil-fuel-based solutions.

## REFERENCE

- [1]. T. A. Dawood, R. Raphael, I. Barwari, and A. Akroot, “Solar Energy and Factors Affecting the Efficiency and Performance of Panels in Erbil / Kurdistan,” *International Journal of Heat and Technology*, vol. 41, no. 2, pp. 304–312, 2023, doi: doi.org/10.18280/ijht.410203.
- [2]. A. Alfari, A. Akroot, S. Alqaed, and F. A. Almeahmadi, “Performance analysis of integrated solar and natural gas combined cycle power plants in high solar potential regions,” *Sci Rep*, vol. 15, no. 1, p. 9181, 2025.
- [3]. T. Ai et al., “Thermodynamic analysis of a CCHP system integrated with a regenerative organic flash cycle,” *Appl Therm Eng*, vol. 202, p. 117833, 2022.
- [4]. A. Piña-Martínez, S. Lasala, R. Privat, V. Falk, and J.-N. Jaubert, “Design of promising working fluids for emergent combined cooling, heating, and power (CCHP) systems,” *ACS Sustain Chem Eng*, vol. 9, no. 35, pp. 11807–11824, 2021.
- [5]. S. Huang, L. Duan, Q. Wang, L. Huang, and H. Zhang, “Thermodynamic analysis of a CCHP system with hydrogen production process by methane reforming enhanced by solar-assisted chemical looping adsorption,” *Appl Therm Eng*, vol. 248, p. 123137, 2024.
- [6]. A. Alsharif, I. Imbayah, A. Abdulraheem, A. M. A. Massoud, and O. N. Elazoomie, “Applicability of Solar Energy in Libyan Southern Cities: Challenges and Difficulties”.

- [7]. R. H. Bindra SP, Soul F, Jabu SD, Allawafi A, Belashher AM, "Potentials and Prospects of Renewables in Libya.," *Prog. Clean Energy*, vol. Vol. 2 Nov, 2015, doi: 10.1007/978-3-319-17031-2\_55.
- [8]. M. M. A. Baka and D. I. Eryildiz, "The Possibility of Developing Existing Residential Buildings by Installing Photovoltaic Modules Case Study: Libya–Zuwarah," *European Journal of Engineering and Technology Research*, vol. 6, no. 4, pp. 45–56, 2021.
- [9]. T. Ai et al., "Thermodynamic analysis of a CCHP system integrated with a regenerative organic flash cycle," *Appl Therm Eng*, vol. 202, p. 117833, Feb. 2022, doi: 10.1016/J.APPLTHERMALENG.2021.117833.
- [10]. A. Akroot and M. Refaei, "Thermodynamic and Exergoeconomic Assessment of a Solar-Assisted Combined Cooling, Heating, and Power System in Antalya, Turkey," *Gazi Üniversitesi Fen Bilimleri Dergisi Part C: Tasarım ve Teknoloji*, p. 1, 2025.
- [11]. Z. Han, W. Han, and J. Sui, "Exergo-environmental cost optimization and thermodynamic analysis for a solar-driven combined cooling and power system," *Energy*, vol. 302, p. 131665, Sep. 2024, doi: 10.1016/J.ENERGY.2024.131665.
- [12]. A. Xu, Y. Wang, T. Song, N. Xie, Z. Liu, and S. Yang, "Thermodynamic analyses of an innovative system combined dehumidification, cooling and heating driven by solar energy," *Energy Convers Manag*, vol. 279, p. 116757, Mar. 2023, doi: 10.1016/J.ENCONMAN.2023.116757.
- [13]. V. K. Yadav, J. Sarkar, and P. Ghosh, "Thermodynamic, economic and environmental assessments of a novel solar-driven combined cooling and power system," *J Clean Prod*, vol. 402, p. 136791, May 2023, doi: 10.1016/J.JCLEPRO.2023.136791.
- [14]. P. Saini, J. Singh, and J. Sarkar, "Thermodynamic, economic and environmental analyses of a novel solar energy driven small-scale combined cooling, heating and power system," *Energy Convers Manag*, vol. 226, p. 113542, Dec. 2020, doi: 10.1016/J.ENCONMAN.2020.113542.
- [15]. A. Akroot, M. Almaktar, and F. Alasali, "The Integration of Renewable Energy into a Fossil Fuel Power Generation System in Oil-Producing Countries: A Case Study of an Integrated Solar Combined Cycle at the Sarir Power Plant," *Sustainability*, vol. 16, no. 11, p. 4820, 2024.
- [16]. M. Wang, J. Wang, P. Zhao, and Y. Dai, "Multi-objective optimization of a combined cooling, heating and power system driven by solar energy," *Energy Convers Manag*, vol. 89, pp. 289–297, Jan. 2015, doi: 10.1016/J.ENCONMAN.2014.10.009.
- [17]. R. Yan, J. Wang, Y. Cheng, C. Ma, and T. Yu, "Thermodynamic analysis of fuel cell combined cooling heating and power system integrated with solar reforming of natural gas," *Solar Energy*, vol. 206, pp. 396–412, Aug. 2020, doi: 10.1016/J.SOLENER.2020.05.085.
- [18]. H. Wu, Q. Liu, Z. Bai, G. Xie, J. Zheng, and B. Su, "Thermodynamics analysis of a novel steam/air biomass gasification combined cooling, heating and power system with solar energy," *Appl Therm Eng*, vol. 164, p. 114494, Jan. 2020, doi: 10.1016/J.APPLTHERMALENG.2019.114494.
- [19]. S. Yang, X. Wang, D. Ma, X. Shen, and X. Zhu, "Thermodynamic-Environmental-Economic Evaluations of a Solar-Driven Supercritical CO<sub>2</sub> Cycle Integrated with Cooling, Heating, and Power Generation," *Energies (Basel)*, vol. 18, no. 8, p. 1995, 2025.
- [20]. M. Nourpour, M. H. Khoshgoftar Manesh, A. Pirozfar, and M. Delpisheh, "Exergy, Exergoeconomic, Exergoenvironmental, Emeryy-based Assessment and Advanced Exergy-based Analysis of an Integrated Solar Combined Cycle Power Plant," *Energy and Environment*, vol. 34, no. 2, pp. 379–406, Mar. 2023, doi: 10.1177/0958305X211063558.
- [21]. J. Wang, Z. Lu, M. Li, N. Lior, and W. Li, "Energy, exergy, exergoeconomic and environmental (4E) analysis of a distributed generation solar-assisted CCHP (combined cooling, heating and power) gas turbine system," *Energy*, vol. 175, pp. 1246–1258, 2019, doi: 10.1016/j.energy.2019.03.147.
- [22]. W. Talal and A. Akroot, "An Exergoeconomic Evaluation of an Innovative Polygeneration System Using a Solar-Driven Rankine Cycle Integrated with the Al-Qayyara Gas Turbine Power Plant and the Absorption Refrigeration Cycle," *Machines*, vol. 12, no. 2, p. 133, Feb. 2024, doi: 10.3390/machines12020133.
- [23]. A. Akroot and A. S. Al Shammre, "Economic and Technical Assessing the Hybridization of Solar Combined Cycle System with Fossil Fuel and Rock Bed Thermal Energy Storage in Neom City," *Processes*, vol. 12, no. 7, p. 1433, Jul. 2024, doi: 10.3390/pr12071433.
- [24]. H. Wu, Q. Liu, Z. Bai, G. Xie, J. Zheng, and B. Su, "Thermodynamics analysis of a novel steam/air biomass gasification combined cooling, heating and power system with solar energy," *Appl Therm Eng*, vol. 164, p. 114494, Jan. 2020, doi: 10.1016/J.APPLTHERMALENG.2019.114494.